The Astrophysical Journal, 598:545–552, 2003 November 20
© 2003. The American Astronomical Society. All rights reserved. Printed in U.S.A.

CHANDRA OBSERVATIONS OF THE DWARF NOVA WX HYDRI IN QUIESCENCE

Rosalba Perna,[1,2] Jonathan McDowell,[2] Kristen Menou,[3,4]
John Raymond,[2] and Mikhail V. Medvedev[5]

Received 2003 June 16; accepted 2003 August 4

ABSTRACT

We report *Chandra* observations of the dwarf nova WX Hyi in quiescence. The X-ray spectrum displays strong and narrow emission lines of N, O, Mg, Ne, Si, S, and Fe. The various ionization states implied by the lines suggest that the emission is produced within a flow spanning a wide temperature range, from $T \sim 10^6$ K to $T \gtrsim 10^8$ K. Line diagnostics indicate that most of the radiation originates from a very dense region, with $n \sim 10^{13}$–10^{14} cm^{-3}. The *Chandra* data allow the first tests of specific models proposed in the literature for the X-ray emission in quiescent dwarf novae. We have computed the spectra for a set of models ranging from hot boundary layers, to hot settling flow solutions, to X-ray–emitting coronae. WX Hyi differs from other dwarf novae observed at minimum in having much stronger low-temperature lines, which prove difficult to fit with existing models, and possibly a very strong, broad O vii line, perhaps produced in a wind moving at a few times 10^3 km s^{-1}. The accretion rate inferred from the X-rays is lower than the value inferred from the UV. The presence of high-velocity mass ejection could account for this discrepancy while at the same time explaining the presence of the broad O vii line. If this interpretation is correct, it would provide the first detection of a wind from a dwarf nova in quiescence.

Subject headings: novae, cataclysmic variables — stars: individual (WX Hydri) — X-rays: stars

1. INTRODUCTION

Cataclysmic variables (CVs) are a class of interacting binaries in which a donor star transfers mass onto a white dwarf (WD) accretor (see Warner 1995 for a comprehensive review). The characteristics of the accretion flow depend mostly on the rate of accretion onto the WD and on the WD magnetic field strength. In nonmagnetic systems ($B \lesssim 10^4$ G), accretion from the donor proceeds through an undisturbed accretion disk, which connects to the WD through a boundary layer (BL) (Patterson & Raymond 1985). When the WD is more strongly magnetized, the accreting material is forced to follow the topology of the field lines before it hits the surface (Aizu 1973).

As a dwarf nova of the SU UMa type, WX Hyi (discovered by Luyten 1932) belongs to the class of nonmagnetic CVs. Its orbital period is 0.0748134 days, and because it does not show eclipses, only an estimated inclination angle of $40° \pm 10°$ is available (Schoembs & Vogt 1981). Schoembs & Vogt (1981) derive a WD mass of 0.9 ± 0.3 $M_\odot$. Normal outbursts occur on average every 11.2 days (Ak, Ozkan, & Mattei 2002). Distance estimates range from 120 pc, based on the correlation between Hβ equivalent width and mass transfer rate, $\dot{M}$ (Patterson 1994), to 265 pc, based on the correlation between period and absolute magnitude during outburst (Warner 1987). We adopt 265 pc because the latter correlation is tighter. Patterson (1984) estimates $\dot{M} = 1.8 \times 10^{16}$ g s^{-1} from the Hβ equivalent width, which would give an X-ray luminosity of 2×10^{33} ergs s^{-1} if half the accretion energy emerges as X-rays. However, Schwope et al. (2002) find an X-ray luminosity of only 4×10^{31} ergs s^{-1} from the *ROSAT* All-Sky Survey data (assuming a 265 pc distance), which yields $\dot{M} \sim 3 \times 10^{14}$ g s^{-1}. K. Long (2003, private communication) finds accretion rates on the order of 10^{15} g s^{-1} from fits of accretion disk models to the UV continuum. The optical emission lines are single-peaked (Schoembs & Vogt 1981), perhaps placing WX Hyi in the SW Sex class of CVs. Strong, rather broad UV emission lines are seen in *IUE* spectra, with the N v line being stronger than is typical of dwarf novae in quiescence (Hassall et al. 1983).

Here we are interested in the structure of the accretion flow in the quiescent state. In quiescence, the accretion rate in the disk is low ($\dot{M} \lesssim 10^{16}$ g s^{-1}), and the disk is too cool to contribute any significant X-ray emission, while on the other hand the BL is expected to be optically thin and thus emit copious amounts of X-rays. According to the standard accretion theory (see, e.g., Lynden-Bell & Pringle 1974), the gravitational energy from the accreting material should reemerge in roughly equal proportions from the disk and the BL. Whereas initial *Einstein* data on quiescent CVs appeared to be consistent with emission from a hot, optically thin BL (Patterson & Raymond 1985), later observations with *Ginga*, *ROSAT*, *ASCA*, and *RXTE* showed that the X-ray luminosity is actually lower than theoretically expected. Several suggestions have been made to solve this "mystery of missing BLs" (see, e.g., Ferland et al. 1982), such as (among others) reflection effects and cooling flows (Done & Osborne 1997) and disruption of the inner disk region by the WD rotation (Ponman et al. 1995), irradiation from the WD (King 1997), or "coronal" evaporation (Meyer & Meyer-Hofmeister 1994).

The presence and structure of BLs (or more generally hot flows) in quiescent CVs is therefore still a subject of debate, and wildly different models have been proposed (see, e.g.,

[1] Harvard Society of Fellows, 74 Mount Auburn Street, Cambridge, MA 02138; rperna@cfa.harvard.edu.
[2] Harvard-Smithsonian Center for Astrophysics, 60 Garden Street, Cambridge, MA 02138; jmcdowell@cfa.harvard.edu, jraymond@cfa.harvard.edu.
[3] Celerity Foundation Fellow.
[4] Virginia Institute of Theoretical Astronomy, and Department of Astronomy, P.O. Box 3818, University of Virginia, Charlottesville, VA 22903; kmenou@virginia.edu.
[5] Department of Physics and Astronomy, Kansas University, Lawrence, KS 66045; medvedev@ku.edu.

Narayan & Popham 1993, hereafter NP93; Meyer & Meyer-Hofmeister 1994; Mahasena & Osaki 1999; Medvedev & Menou 2002). While all the models can account for the *total* observed X-ray luminosity, each of them, however, makes very specific predictions for the physical conditions within the flow and hence the resulting temperature and density profiles. As shown in a number of papers (among the most recent ones are Pradhan 2000; Mauche, Liedahl, & Fournier 2001; Perna, Raymond, & Narayan 2000; Menou, Perna, & Raymond 2001; Porquet et al. 2002; Dubau & Porquet 2002; and Szkody et al. 2002), a powerful way to constrain the characteristics of hot, X-ray–emitting flows is through the relative intensities of emission lines produced within them. The high resolution of *Chandra* gives us the opportunity, for the first time, to resolve relative line intensities and perform such an analysis.

In this paper, we report *Chandra* observations of the dwarf nova WX Hyi in quiescence. Its X-ray spectrum shows many lines from different ionization states of N, O, Ne, Mg, Si, S, and Fe. First, we use line diagnostics to set overall constraints on the range of temperatures and densities spanned by the flow. Second, we compute X-ray spectra for different types of accretion flow structures and test them against our data. The comparison shows that none of the models provides an adequate fit to the entire emission-line spectrum, in that more plasma must be present at relatively low temperatures than predicted by the models. A cooling flow model (used by Mukai et al. 2003 to model spectra of nonmagnetic CVs) is consistent with the short-wavelength spectra but fails to reproduce the strength of the O VII line. This line is much stronger and broader than in the objects studied by Mukai et al., and we consider the intriguing possibility that it might be produced in a wind from the accretion flow.

2. DATA ANALYSIS

WX Hyi was observed on-axis by the *Chandra X-Ray Observatory*'s ACIS-S detector and High Energy Transmission Grating (HETG) on 2002 July 25 and 28 (observation IDs 3721 and 2760), with effective exposure times after standard processing of 48,366 and 49,266 s, respectively. Optical data provided by the AAVSO show that WX Hyi was in quiescence during both observations, with an outburst 4 days after the second observation, on August 2. The previous detected outburst was 20 days before our first observation. Examination of the background light curves shows no significant variability due to dropouts or flares. The *destreak* algorithm was applied to remove electronic noise from the noisier S4 chip, and the standard extraction parameters were used to obtain dispersed count spectra. The -1 and $+1$ orders for both observations were co-added to obtain summed HEG and MEG spectra (high-energy and medium-energy grating, respectively). There was no significant difference in the spectra between the two exposures. The secular degradation of the ACIS quantum efficiency was taken into account using the *acisabs* model while making the response files.

The spectra were grouped to a signal-to-noise ratio (S/N) of 2 per bin. Initial attempts to model the lines in the merged spectrum with the CIAO fitting program SHERPA, using both global model fits and fits to individual lines with a Gaussian line model and polynomial fits to the local continuum, gave unsatisfactory, poorly constrained results for the weaker lines. Instead, we determined line fluxes by simple integration of the counts in a band around each line, subtracting the continuum contribution using two methods: comparison with counts in nearby wavelength bands and subtraction of a broken–power-law fit to the global continuum. These two methods gave consistent results and are in reasonable agreement with the Gaussian line fits in the case of the strongest lines. In addition, measurements of the stronger lines in the individual single-order exposures give consistent results. Line flux measurements are presented in Table 1, together with probable identifications. The errors in Table 1 are 1 σ statistical uncertainties computed for the line and continuum counts using the Gehrels (1986) approximation suitable for low-count Poisson statistics.

The cleanest X-ray line is the O VIII resonance line at 18.967 Å. Its width is $\sim$900 km s^{-1} (FWHM) after correction for the instrument profile. Correcting for the 40° inclination, the intrinsic width is $\sim$1400 km s^{-1}. While this is similar to the widths ($\sim$1200 km s^{-1}) of the UV lines, the wings ($\sim$4000 km s^{-1}) apparent in the UV line profiles (K. Long 2003, private communication) are absent. The

TABLE 1
LINE SUMMARY

Element	λ[a] (Å)	HEG Flux (10^{-14} ergs cm^{-2} s^{-1})	MEG Flux (10^{-14} ergs cm^{-2} s^{-1})
Fe XXVI........	1.78	12.5 ± 6.4	...
Fe XXV.........	1.85	54.1 ± 7.1	67 ± 20
Fe Kα	1.94	10.0 ± 3.9	...
S XVI...........	4.73	4.5 ± 1.8	4.1 ± 0.9
S XV............	5.05	<6.0	2.8 ± 1.1
Si XIV..........	6.19	6.3 ± 0.9	5.6 ± 0.5
Si XIII..........	6.65	1.0 ± 0.7	0.73 ± 0.44
Fe XXIV........	8.00	1.4 ± 0.4	0.5 ± 0.2
Mg XII	8.42	2.1 ± 0.4	2.3 ± 0.3
Mg XI	9.17	<1.0	0.63 ± 0.3
	9.23	...	0.24 ± 0.1
	9.31	...	0.22 ± 0.2
Ne X	10.24	1.4 ± 1.5	0.5 ± 0.2
Fe XXIV........	10.62[b]	1.9 ± 0.6	1.8 ± 0.3
	10.66[b]	0.9 ± 0.4	1.7 ± 0.3
	11.05	1.3 ± 0.7	0.85 ± 0.3
	11.17	2.4 ± 0.8	2.3 ± 0.3
Fe XXIII	11.73	1.5 ± 0.7	1.1 ± 0.2
Fe XXII.........	11.77	1.3 ± 0.7	1.1 ± 0.3
	11.92	<1.3	0.75 ± 0.4
Ne X	12.13	4.3 ± 1.0	5.0 ± 0.6
Ne IX	13.44	...	2.3 ± 0.5
	13.55	...	1.7 ± 0.5
	13.70	...	<0.8
Fe XVII.........	15.03	...	2.6 ± 0.6
	17.05	...	1.9 ± 0.6
	17.10	...	<1.1
O VIII..........	18.96	...	7.0 ± 1.3
O VII...........	21.60[c]	...	3.9 ± 2.1
O................	21.80[c]	...	...
Fe XXIV........	21.97[c]	...	...
N VII...........	24.74	...	4.5 ± 1.5

[a] The center of the lines are taken at the theoretical values obtained from the atomic database distributed with CIAO, except for the blend of Fe XXII and Fe XXIII near 11.7 Å, where we use wavelengths measured from solar spectra (Doschek & Cowan 1984).
[b] These two lines are blended in MEG.
[c] These three lines are blended.

inclination-corrected line width is $\lesssim\frac{1}{3}$ the Keplerian velocity near the WD surface.

3. CONSTRAINTS ON THE CHARACTERISTICS OF THE ACCRETION FLOW FROM THE X-RAY SPECTRUM

3.1. *Line Diagnostics*

The X-ray spectrum, including both the MEG and HEG observations, is displayed in Figure 1. The spectrum shows a smooth continuum with strong emission lines, particularly from the H- and He-like ions of O, Mg, Ne, Si, and Fe, as well as from all the Fe L-shell complex (Fe XVII–Fe XXIV). The presence of this variety of ionization states indicates emission from a plasma distributed over a wide range of temperatures, from $T \sim 10^6$ K, necessary to have some contribution to the O VII line, up to $T \sim 10^8$ K, a temperature at which the ion Fe XXVI is most abundant in equilibrium (without strong photoionizing radiation).

From the X-ray spectrum in Figure 1, one can see that the O VII line profile appears to be wider than those of O VIII and the other lines, although it is clearly noisy. The profile, which is separately displayed in Figure 2, seems to consist of narrow O VII resonance and forbidden lines on top of a broad feature perhaps 5000 km s^{-1} wide. Some of the noise level results from the presence of bad columns in the $+1$ order of the MEG, which are broadened by dithering. However, careful examination of the counts in the -1 order in the individual exposures indicates that the broad feature is probably real, although details of the structure are questionable. Note that the effective area changes rapidly in this wavelength range, making the number of counts in the blueshifted part of the feature more significant. It is difficult to determine an unambiguous value for the uncertainty, in that different choices for spectral binning yield different estimates of the significance of the feature. There are several lines of calcium near this wavelength, but comparison with iron lines formed at the same temperatures indicates that the calcium lines are too weak to account for the observed structure. It should be noted, however, that there appears to be also a feature around 20.3 Å for which we have no identification.

If the broad O VII component is genuine, the lack of broad components in the other lines suggests that the high-velocity material only appears in low-ionization species. The lack of this component in N VII must be due to the small number of counts in that line. The line width is comparable to or larger than the widths ($\sim$1200 km s^{-1}) of the UV Lines (K. Long 2003, private communication), so the broad O VII might originate in the innermost part of the disk or in a wind.

As a first attempt to constrain the physical conditions in the accretion flow, we use the diagnostics provided by the He-like triplet line ratios, which have been widely used in analyses of the solar plasma (Gabriel & Jordan 1969; Mewe & Schrijver 1978; Doyle 1980; Pradhan & Shull 1981). In particular, the ratio $R \equiv f/i$ between the forbidden line f and the intercombination line i is a strong function of the density at high densities, because of the suppression of the forbidden lines with increasing density. The ratio R is typically on the order of a few at low densities and rapidly drops at densities larger than a critical value n_c that increases with Z, ranging from $n_c \approx 6 \times 10^8$ cm^{-3} for C, to $n_c \approx 3 \times 10^{17}$ cm^{-3} for Fe (see, e.g., Porquet et al. 2001). We find the 1 σ upper limits $R < 0.47$ and $R < 0.92$ for Ne[6] and Mg, respectively. The $1s2s\ ^3S$–$1s2p\ ^3P_1$ transition, however, is driven not only by collisions, but also by UV radiation, so that in gas near a 30,000 K blackbody the f/i ratio will be in the high-density limit for elements through Mg (Mauche 2002). We do not know the WD temperature for WX Hyi. K. Long (2003, private communication) has fitted UV continua of WX Hyi observed by the Hopkins Ultraviolet Telescope and the *Hubble Space Telescope* Goddard High Resolution Spectrograph (GHRS) with combinations of WD and accretion disk spectra and typically finds WD temperatures above 20,000 K. The f/i ratios of O VII, Ne IX, and Mg XI are probably dominated by UV radiation, but the f/i ratio for Si XIII should be dominated by collisions, even if the entire UV continuum in the Hopkins Ultraviolet Telescope wavelength range arises from the WD. Unfortunately, we are unable to obtain a reliable measurement of the Si XIII ratio.

Another useful plasma diagnostic is the ratio $G \equiv (i+f)/r$, where r is the resonance line. This is sensitive to the ionization state of the gas and the electron temperature. When the resonance line is strong compared to the forbidden and the intercombination line ($G \lesssim 1$), the plasma is collision-dominated. On the other hand, a plasma in which photoionization is important will have a weaker resonance line. Values of $G > 4$ are typically considered to be indicative of a photoionization-dominated plasma (see, e.g., Porquet et al. 2001). For O, Si, and S, we found that the i, r, and f lines were not sufficiently well resolved to allow a reliable estimate of the G-value. In the cases of Mg and Ne, we were able to set the 1 σ upper limits $G < 0.73$ and $G < 1.08$, respectively. This indicates that photoionization is not dominant.

A useful density diagnostic is provided by the ratio between the 17.10 and the 17.05 Å lines of the ion Fe XVII, which is less sensitive to UV radiation than are the He-like line ratios (Mauche et al. 2001). The Fe XVII ratio $I(17.10)/I(17.05)$ is found to be $\lesssim$0.6 (at the 1 σ level) for WX Hyi. For a collisionally dominated plasma, this value suggests a density $n \gtrsim 3 \times 10^{13}$ cm^{-3} in the relatively cooler region [$T \sim (3$–$6) \times 10^6$ K] where Fe XVII is produced. A comparable density is implied by the best value of the ratio between the 11.92 and the 11.77 Å lines of Fe XXII, which is found to be 0.68 ± 0.4 in our data. Accounting for the error in the measurement, the 1 σ confidence level for the density ranges between 10^{13} and 10^{14} cm^{-3}. As discussed by Mauche, Liedahl, & Fournier (2003), this density determination is very insensitive to temperature and photoexcitation.

3.2. *Comparison with Specific Models for the X-Ray Emission*

The physics, and hence the density-temperature structure, of BLs is still poorly understood. Only a few models have been proposed, and they have been primarily tested on their ability to account for the *total* observed X-ray and UV radiation. The *Chandra* observations of the X-ray emission, by resolving lines, allow us to set much tighter constraints on the models, because of the high sensitivity of the relative line

[6] It should be noted that the intercombination line of Ne is not very clean and might have some contamination from Fe XIX that is not possible to quantify.

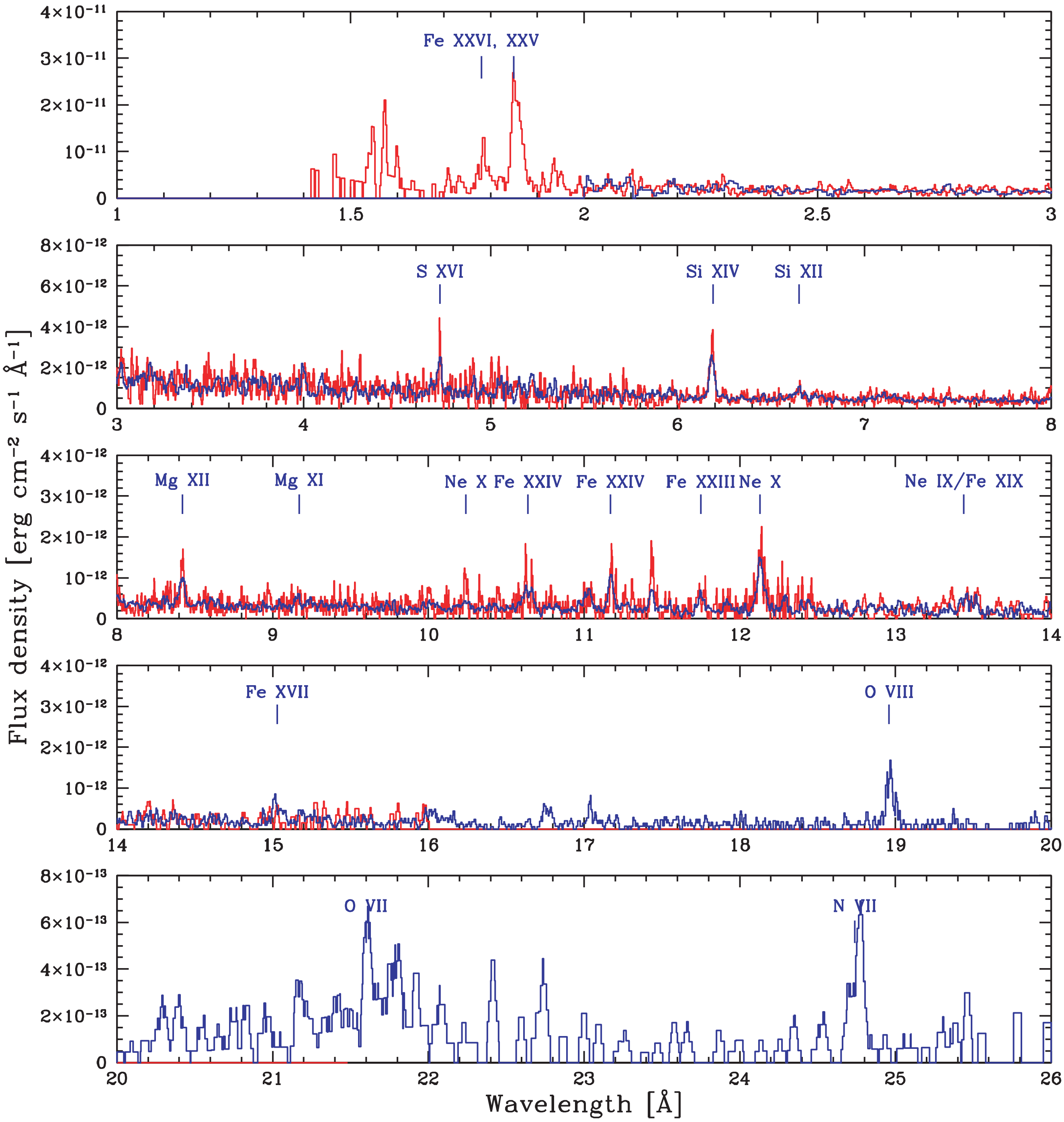

FIG. 1.—*Chandra* spectrum of the dwarf nova WX Hyi in quiescence. The spectrum has been binned so that each bin has S/N = 2. Both the MEG (*blue*) and the HEG (*red*) spectra are displayed.

intensities to the temperature and density profiles characterizing the flow. Here we consider five types of models proposed in the literature to explain the origin of the quiescent X-ray emission of CVs. For each of them, we compute the expected X-ray spectrum, using the temperature and density profiles that they predict, and compare the spectra with our observations. The cooling flow model has been implemented in the XSPEC package (Arnaud 1996). For the other models, we compute the emissivity of the medium by using the atomic rate packages of the shock model code described by Raymond (1979), modified with updated atomic rates, as in Cox & Raymond (1985). This package has the disadvantage that some Fe L-shell multiplets that are resolved in our spectra are computed as single lines. The package also lacks recent improvements to the atomic rates of the more complex Fe ions. It computes an ionization balance that is quite similar to that of Mazzotta et al. (1998) in ionization equilibrium. The advantage of the code is that it allows us to compute time-dependent ionization and to include photoionization. It includes dielectronic recombination satellite lines and the contributions of recombination to excited levels for the spectra of H- and He-like ions. Overall,

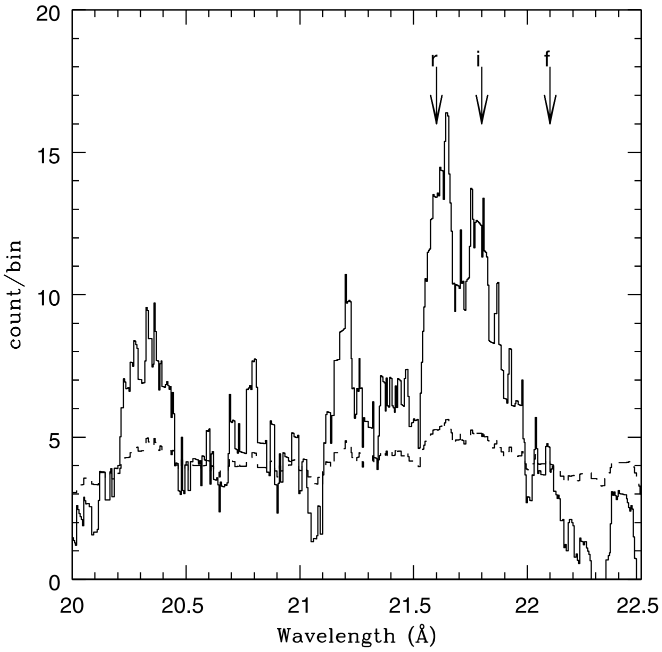

FIG. 2.—Details around the O VII line complex, showing flux smoothed with a 0.125 Å boxcar (*solid line*). The dashed line indicates combined uncertainty from background and count statistics. The *r*, *i*, and *f* lines of O VII are indicated. Excess flux between 21.0 and 21.5 Å appears real and may represent blueshifted velocity components of O VII.

the predictions should be reasonably accurate for most of the strong lines: those of H- and He-like ions, Fe XVII, and Fe XXIV. For the models presented here, we included the effects of photoionization by the X-ray radiation produced within the flow itself, although this turned out to have little effect on the emission lines. For a proper comparison with the data, the computed X-ray spectra were then convolved with the response matrices and effective areas of the *Chandra* detectors. In particular, we used the HEG detector for $\lambda \leq 3$ Å and the MEG detector for $\lambda > 3$ Å.

Cooling flow (Fig. 3*a*).—A cooling flow model, based on Mushotzky & Szymkowiak (1988), has been implemented in XSPEC with the routine MKCFLOW. Its basic assumption is of steady state, isobaric, radiative cooling. The two main parameters are the maximum temperature, $T_{\rm max}$, and the overall normalization, which directly relates to the mass accretion rate. Mukai et al. (2003) showed that cooling flow models provide a good representation of the X-ray spectral properties of nonmagnetic CV systems. A fit to our data with the model MKCFLOW is shown in Figure 3*a*. We find that the fit is acceptable at short wavelengths but poorly constrained, with the maximum temperature parameter at a value of 20 keV, uncertain by a factor of 2, and the column density $N_{\rm H} = (2 \pm 2) \times 10^{20}$ cm^{-2} (basically consistent with zero). The value of the temperature is consistent with the Fe XXVI/Fe XXV ratio that gives an upper limit of 10 keV. Note that this ratio is about $\frac{1}{7}$ in WX Hyi as opposed to $\frac{3}{4}$ in U Gem (Szkody et al. 2002), implying a corresponding lower temperature of WX Hyi. The value of $\dot{M}$ implied by the cooling model is $\sim 2 \times 10^{14}$ g s^{-1} for $T_{\rm max} = 20$ keV (assuming that half of the X-rays are absorbed by the WD). This is about a factor of 5 smaller than the value found by K. Long (2003, private communication) from fits of disk models to the UV continuum. While the system is by definition variable, it is not surprising that the X-ray luminosity is less than expected from $\dot{M}$ farther out in the disk. Possible interpretations are that $\dot{M}$ decreases inward in the disk as material builds up for the next outburst, that some material and energy is lost to a wind, or that some energy is advected to the WD surface and reemitted in the UV.

Overall, the cooling flow model appears to account reasonably well for the continuum and the line strengths in the short-wavelength region of the spectrum, but it underpredicts the emission at long wavelengths. In particular, it is not able to account for the emission from the O VII line, which in WX Hyi is significantly stronger than in the objects studied by Mukai et al. (2003).

Hot BL (Fig. 3*b*).—NP93 describe detailed models for thin-disk BLs in CVs. A key element of their theory is the role of heat advection, which, they show, allows BLs at low accretion rates to be radially thicker and significantly hotter than those at higher accretion rates. We have used the profiles of density and temperature corresponding to the model with $\dot{M} = 2 \times 10^{15}$ g s^{-1}, which is the closest to the accretion rate in our system. The behavior of the low-temperature region closest to the WD surface cannot be read from the plots in NP93, but this is a small fraction of the total X-ray luminosity and may be neglected. We note that the comparison with this particular solution should be interpreted with caution, as temperature and density do not simply scale with accretion rate. Figure 3*b* shows a comparison between our data and the X-ray spectrum that we computed for this BL solution. The spectrum has been rescaled to match the continuum. If the density profile were to scale linearly with the accretion rate, the data would imply a value of $\dot{M}$ of about 2×10^{14} g s^{-1}. As the figure shows, this model predicts substantially more emission than the cooling flow in the O VII and O VIII lines. This is a result of the fact that the BL solution of NP93 predicts an increase of the density in the outer, colder regions of the flow, where the oxygen emission peaks. However, the reasonable agreement between the observed and predicted low-temperature lines is partly fortuitous, in that NP93 assumed bremsstrahlung cooling, while the actual line cooling rate at the temperatures where the O VII, O VIII, and Fe XVII lines are formed is nearly an order of magnitude higher. Thus, if NP93 had used a cooling rate consistent with the lines we observe, their model would have predicted emission weaker by an order of magnitude.

Coronal siphon flow (Fig. 3*c*).—Meyer & Meyer-Hofmeister (1994) investigated a model based on the interaction between a cool disk and a hot corona above it via thermal conduction. They showed that, in these conditions, a coronal " siphon flow " can develop. This evaporates mass from the disk that is partly accreted onto the WD and partly lost to a wind. The solutions for this model are uniquely determined once the viscosity parameter α for the flow is specified.[7] We varied the value of this parameter to find the best-fit coronal flow solution to our data. The resulting X-ray spectrum predicted for the coronal siphon flow is shown in Figure 3*c*. As can be seen, this model falls short of producing enough emission in the long-wavelength region of the spectrum. This is a consequence of the fact that this

[7] Under the conditions in which the radiative energy loss in the corona is small compared to conductive energy loss toward the lower boundary and the wind loss, the radial solutions for T and ρ are independent of $\dot{M}$ for a given WD mass (Meyer & Meyer-Hofmeister 1994).

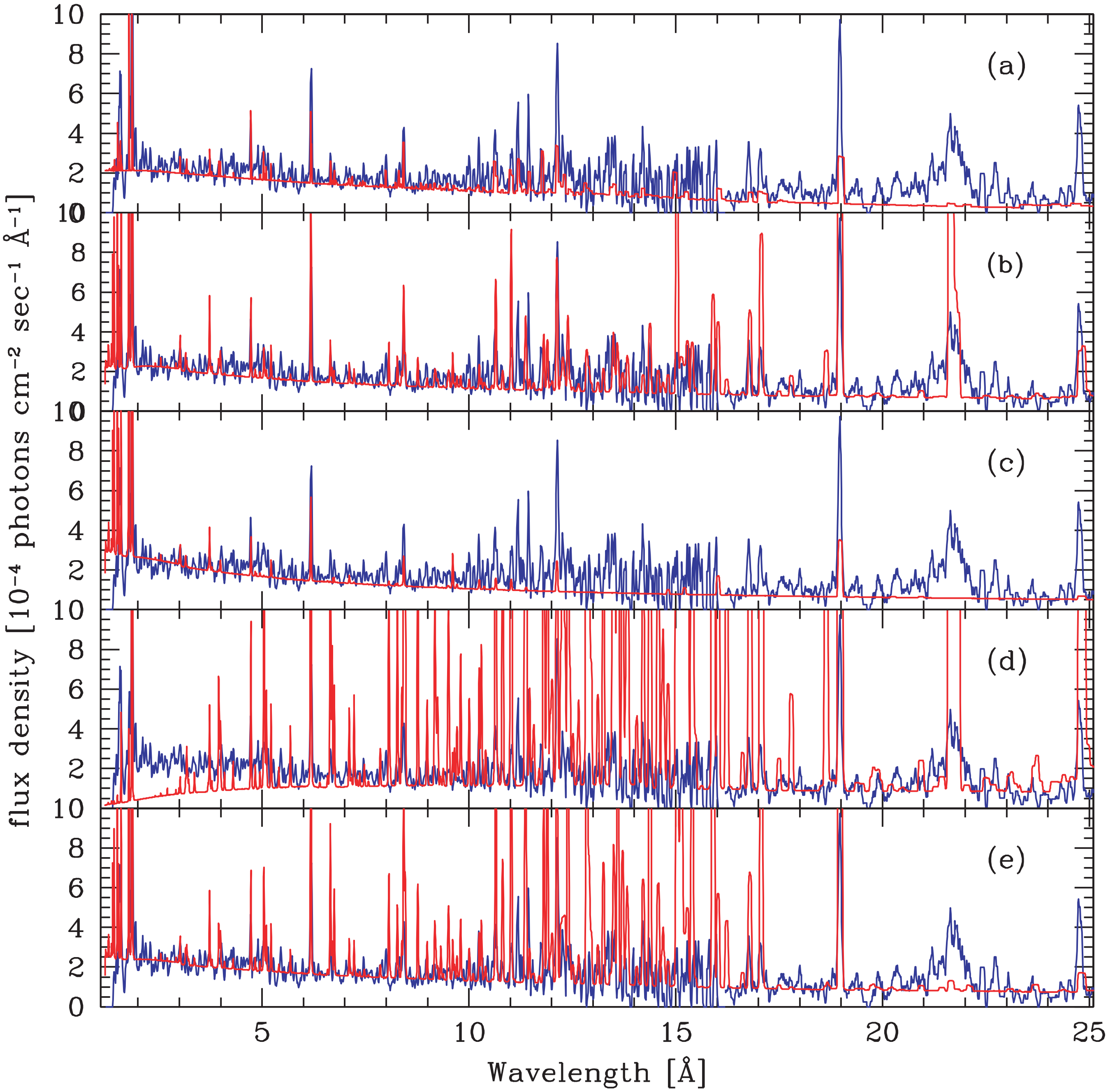

FIG. 3.—Quiescent emission of WX Hyi as seen by *Chandra* (*blue*), compared to theoretical spectra computed for several models (*red*): (*a*) cooling flow (Mushotzky & Szymkowiak 1988); (*b*) hot BL (NP93); (*c*) coronal siphon flow (Meyer & Meyer-Hofmeister 1994); (*d*) hot X-ray–emitting corona (Mahasena & Osaki 1999); and (*e*) hot settling flows (Medvedev & Menou 2002).

solution predicts a radial temperature profile $T \propto r^{-1}$ and a run of density that is a very steep function of the radius, $n \propto r^{-3}$. This implies that there is relatively little mass at the lower temperatures, at which the longer wavelength emission is generated.

X-ray–emitting corona (Fig. 3*d*).—Mahasena & Osaki (1999) constructed steady state solutions of an X-ray–emitting corona, including the effect of thermal conduction. We have used the density and temperature profiles shown in their Figure 1 for an accretion rate $\dot{M} = 10^{15}$ g s^{-1} and calculated the corresponding X-ray spectral emission. It was not possible to read numbers from their plot for the region below 6×10^6 K, so we computed a matching solution that neglected the rotation and infall velocities, both of which are small in this region. The result is compared to the data in Figure 3*d*. This comparison should also be taken with caution, because the value of the accretion rate is not precisely tuned to match that of WX Hyi. This coronal model, which transports most of the accretion luminosity to a cool, thin, conduction-dominated layer near the WD surface and radiates it there, produces emission lines that are far too strong and a continuum that is much too soft. The higher accretion rate model of Mahasena & Osaki, $\dot{M} = 10^{16}$ g s^{-1}, did a much better job matching the *Chandra* spectrum of

U Gem (Szkody et al. 2002),[8] because it is closer to the cooling flow solution, which matches that spectrum quite well (Mukai et al. 2003). However, the cooling model predicts too little emission in the low-temperature lines to match the WX Hyi spectrum. The density in the region where the Fe XXII lines are produced is about 3×10^{14} cm^{-3} in this model, a few times higher than the density-sensitive line ratio indicates.

Hot settling flow solutions (Fig. 3*e*).—Following Medvedev & Narayan (2001), Medvedev & Menou (2002) presented solutions for hot accretion onto unmagnetized, rotating WDs. Together with the accretion rate, the WD rotation rate is an important parameter in these models, because viscously mediated losses of rotational energy by the WD constitute an additional source of energy powering the X-ray emission from the flow (see Medvedev & Menou 2002 for examples). To calculate the hot flow models we used the numerical relaxation code, which solves height-integrated, two-temperature hydrodynamic equations with high spatial resolution, providing accurate solutions even deep inside the BL. This is the same code that has previously been used by Medvedev & Menou (2002), except for the cooling part, which now also incorporates (in addition to bremsstrahlung) the emission-line cooling in the form $\bar{q}_{\rm line} = 6.6 \times 10^{-22} T_5^{-0.73} n_e n_{\rm H}$ ergs cm^{-3} s^{-1}, which is a good approximation above $T = 10^5$ K, where $T_5 = T/(10^5\ {\rm K})$ (Raymond, Cox, & Smith 1976). At the high densities of the WX Hyi BL, quenching of UV lines reduces the cooling rate below 10^6 K, but here we are concerned only with lines formed above 10^6 K. In our present solutions, we have chosen the outer boundary of the flow to be at radius $R = 10^2 R_{\rm WD}$, which is realistic. We have computed hot settling flow models appropriate for WX Hyi. Absent any observational constraint on the WD rotation in this system, we have computed a variety of models, with values for the spin parameter, s (the angular velocity of the WD in units of the Keplerian angular velocity), ranging from 0.03 to 0.3. The accretion rate in the models was adjusted so that the observed X-ray luminosity is reproduced in each case (see Medvedev & Menou 2002 for details). The required value was on the order of 10^{15} g s^{-1}.

We found that the X-ray spectrum predicted by the hot settling flow solution greatly overpredicts the X-ray line emission with respect to our observations. Figure 3*e* shows the spectrum predicted by this solution for the case $s = 0.03$. As s increases, line emission becomes even more pronounced. Therefore, unless optical depth effects become sufficiently important to suppress line emission, this solution does not appear to reproduce the observations well.

4. CONCLUSIONS

The *Chandra* observations of the dwarf nova WX Hyi in quiescence show resolved spectral lines produced within the accretion flow. Line diagnostics have allowed us to set constraints on the characteristics of the hot flow, showing that gas densities are very high, $n \sim 10^{13}$–10^{14} cm^{-3}, and span a wide range of temperatures, $T \sim 10^6$–10^8 K.

The spectrum of WX Hyi shows some unusual features if compared to the spectra of the objects in the same class studied by Mukai et al. (2003). Lines in the longer wavelength region of the spectrum are relatively stronger. The O VII line especially cannot be accounted for by the cooling flow model used by Mukai et al. to fit the spectra of this type of object.

The *Chandra* data allow the first tests of specific models proposed in the literature for the X-ray emission in quiescent dwarf novae. We have computed the spectra for a set of models ranging from hot BLs, to hot settling flows solutions, to X-ray–emitting coronae. While most of these models can reproduce well the shape of the continuum, none of them can fully account for the relative line strengths over the entire spectral range. Most coronal models fall short of predicting enough radiation at longer wavelengths, although a thermal conduction–dominated BL predicts too much long-wavelength emission. Hot accretion solutions tend to overpredict the short-wavelength emission. It is possible, but far from obvious, that some combination of these models, perhaps with thermal conduction present but reduced by a magnetic field, might match the observations.

Given the difficulties of the existing models, it is possible that somewhat different physical processes dominate the BL flow. In particular, it has been suggested that magnetic flux tubes rise above the disk surface and produce X-rays in the same manner as solar flares (Galeev, Rosner, & Vaiana 1979). While X-ray emission from the disk as a whole is excluded by the X-ray light curve of OY Car, which limits much of the X-ray emission to the immediate vicinity of the WD (Ramsay et al. 2001), the BL is likely to be magnetically dominated. The BL itself is stable against magnetorotational instability (Balbus & Hawley 1991), but magnetic flux generated just beyond the BL diffuses into it, and the toroidal component is strongly amplified by the enormous shear (Armitage 2002; Steinacker & Papaloizou 2002). Lacking a more definite prediction, one might expect a power-law distribution of X-ray flare energies, as on the Sun (UeNo et al. 1997), and perhaps a significant contribution from flares that reach modest temperatures (see, e.g., Raymond 1990). Detailed models require Monte Carlo simulations of flare energies, intervals between flares, and physical processes such as thermal conduction, and they are beyond the scope of this paper. It is possible, however, that some combination of parameters can be found to roughly match the data.

It is therefore possible that the BL is better described as a collection of impulsive magnetic reconnection events than as a smooth fluid flow. An implication of this idea is that a significant amount of mass may be expelled as a wind. Solar flares are often accompanied by coronal mass ejections (CMEs), and on average the CMEs carry somewhat more kinetic energy than the flares emit as radiation. Thus, mass ejections could easily account for the factor of 3 or so discrepancy between the accretion rates estimated from the UV and X-ray spectra. Thus far, winds from CVs have only been detected in high-$\dot{M}$ systems. It has recently been shown that these winds are not driven by radiation pressure alone (Mauche & Raymond 2000; Proga 2003). There is as yet no way to determine whether large-scale fields, as in Proga's models, or small-scale, CME-like eruptions dominate the wind. Winds from low accretion rate systems are difficult to detect because of the high ionization state expected.

Assuming that the broad component of the O VII emission (§ 2) is real, it could be formed in the wind hypothesized in the previous paragraph. A simple estimate of the mass-loss

[8] Note that there is a typo in Szkody et al. (2002) in reporting the higher value of the accretion rate used as $\dot{M} = 10^{15}$ g s^{-1}, rather than $\dot{M} = 10^{16}$ g s^{-1}.

rate from a surface corresponding to the WD circumference and the BL width ($\sim 10^8$ cm) with a density $n \sim 3 \times 10^{13}$ cm^{-3} (as required to match the O VII luminosity) and a speed v of 3000 km s^{-1} yields about 2×10^{15} g s^{-1}, or more than the total $\dot{M}$ inferred from the UV spectra. Thus, in order to identify the broad O VII emission with a wind, we require a filling factor on the order of 0.1. With this filling factor, one would in fact need a density $\sim 10^{1/2}$ larger to keep the emission measure ($\propto n^2 V$) of the O VII line at the observed value. The accretion rate $\dot{M} \propto nvA$ (A being the area) would then be $\sim 10^{1/2}$ smaller, consistent with the value inferred from the UV observations. One must be cautious about a wind interpretation both because of the low statistical quality of the O VII profile and because a wide O VII profile might arise from Keplerian rotation of the inner disk just outside the BL. However, a wind of moderate ionization state does provide an appealing explanation for the difference between the accretion rates derived from UV and X-ray observations.

We thank the referee, Chris Mauche, for his careful review of our manuscript and very useful comments. In this research, we have used, and acknowledge with thanks, data from the AAVSO International Database, based on observations submitted to the AAVSO by variable star observers worldwide. This analysis was supported by the *Chandra* grant GO2-3032X to the Smithsonian Astrophysical Observatory and by the Celerity Foundation.

REFERENCES

Aizu, K. 1973, Prog. Theor. Phys., 49, 1184
Ak, T., Ozkan, M. T., & Mattei, J. A. 2002, A&A, 389, 478
Armitage, P. J. 2002, MNRAS, 330, 895
Arnaud, K. A. 1996, in ASP Conf. Ser. 101, Astronomical Data Analysis Systems V, ed. G. H. Jacoby & J. Barnes (San Francisco: ASP), 17
Balbus, S. A., & Hawley, J. F. 1991, ApJ, 376, 214
Cox, D. P., & Raymond, J. C. 1985, ApJ, 298, 651
Done, C., & Osborne, J. P. 1997, MNRAS, 288, 649
Doschek, G. A., & Cowan, R. D. 1984, ApJS, 56, 67
Doyle, J. G. 1980, A&A, 87, 183
Dubau, J., & Porquet, D. 2002, in New Visions of the X-Ray Universe in the *XMM-Newton* and *Chandra* Era, ed. F. Jansen (ESA SP-488; Noordwijk: ESTEC), in press
Ferland, G. J., Langer, S. H., MacDonald, J., Pepper, G. H., Shaviv, G., & Truran, J. W. 1982, ApJ, 262, L53
Gabriel, A. H., & Jordan, C. 1969, MNRAS, 145, 241
Galeev, A. A., Rosner, R., & Vaiana, G. S. 1979, ApJ, 229, 318
Gehrels, N. 1986, ApJ, 303, 336
Hassall, B. J. M., Pringle, J. E., Schwarzenberg-Czerny, A., Wade, R. A., Whelan, J. A. J., & Hill, P. W. 1983, MNRAS, 203, 865
King, A. R. 1997, MNRAS, 288, L16
Luyten, W. 1932, Astron. Nachr., 245, 211
Lynden-Bell, D., & Pringle, J. E. 1974, MNRAS, 168, 603
Mahasena, P., & Osaki, Y. 1999, PASJ, 51, 45
Mauche, C. W. 2002, in ASP Conf. Ser. 261, The Physics of Cataclysmic Variables and Related Objects, ed. B. T. Gänsicke, K. Beuermann, & K. Reinsch (San Francisco: ASP), 113
Mauche, C. W., Liedahl, D. A., & Fournier, K. B. 2001, ApJ, 560, 992
———. 2003, ApJ, 588, L101
Mauche, C. W., & Raymond, J. C. 2000, ApJ, 541, 924
Mazzotta, P., Mazzitelli, G., Colafrancesco, S., & Vittorio, N. 1998, A&AS, 133, 403
Medvedev, M. V., & Menou, K. 2002, ApJ, 565, L39
Medvedev, M. V., & Narayan, R. 2001, ApJ, 554, 1255
Menou, K., Perna, R., & Raymond, J. C. 2001, ApJ, 549, 509
Mewe, R., & Schrijver, J. 1978, A&A, 65, 99
Meyer, F., & Meyer-Hofmeister, E. 1994, A&A, 288, 175
Mukai, K., Kinkhabwala, A., Peterson, J. R., Kahn, S. M., & Paerels, F. 2003, ApJ, 586, L77
Mushotzky, R. F., & Szymkowiak, A. E. 1988, in Cooling Flows in Clusters and Galaxies, ed. A. C. Fabian (Dordrecht: Kluwer), 53
Narayan, R., & Popham, R. 1993, Nature, 362, 820 (NP93)
Patterson, J. 1994, PASP, 106, 209
Patterson, J., & Raymond, J. C. 1985, ApJ, 292, 535
Perna, R., Raymond, J., & Narayan, R. 2000, ApJ, 541, 898
Ponman, T. J., Belloni, T., Duck, S. R., Verbunt, F., Watson, M. G., Wheatley, P. J., & Pfeffermann, E. 1995, MNRAS, 276, 495
Porquet, D., Mewe, R., Dubau, J., Raassen, A. J. J., & Kaastra, J. S. 2001, A&A, 376, 1113
Porquet, D., Mewe, R., Kaastra, K. S., Dubau, J., & Raassen, A. J. J. 2002, in New Visions of the X-Ray Universe in the *XMM-Newton* and *Chandra* Era, ed. F. Jansen (ESA SP-488; Noordwijk: ESTEC), in press
Pradhan, A. K. 2000, in Atomic Data Needs for X-Ray Astronomy, ed. M. A. Bautista, T. R. Kallman, & A. K. Pradhan (NASA CP-2000-209968), 69
Pradhan, A. K., & Shull, J. M. 1981, ApJ, 249, 821
Proga, D. 2003, ApJ, 585, 406
Ramsay, G., et al. 2001, A&A, 365, L288
Raymond, J. C. 1979, ApJS, 39, 1
———. 1990, ApJ, 365, 387
Raymond, J. C., Cox, D. P., & Smith, B. W. 1976, ApJ, 204, 290
Schoembs, R., & Vogt, N. 1981, A&A, 97, 185
Schwope, A. D., Brunner, H., Buckley, D., Greiner, J., Heyden, K.v.d., Neizvestny, S., Potter, S., & Schwarz, R. 2002, A&A, 396, 895
Steinacker, A., & Papaloizou, J. C. B. 2002, ApJ, 571, 413
Szkody, P., Nishikida, K., Raymond, J. C., Seth, A., Hoard, D. W., Long, K. S., & Sion, E. M. 2002, ApJ, 574, 942
UeNo, S., Mineshige, S., Negoro, H., Shibata, K., & Hudson, H. S. 1997, ApJ, 484, 920
Warner, B. 1987, MNRAS, 227, 23
———. 1995, Cataclysmic Variable Stars (Cambridge: Cambridge Univ. Press)